CARBON 48 (2010) 1867–1875

available at www.sciencedirect.com

ScienceDirect

journal homepage: www.elsevier.com/locate/carbon

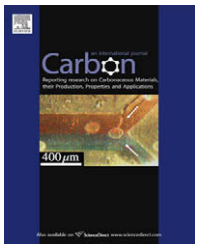

Temperature and pressure dependence of molecular adsorption on single wall carbon nanotubes and the existence of an "adsorption/desorption pressure gap"

Dmitry V. Kazachkin [a,b], *Yoshifumi Nishimura* [c], *Stephan Irle* [c], *Xue Feng* [a,d], *Radisav Vidic* [d], *Eric Borguet* [a,*]

[a] *Department of Chemistry, Temple University, Philadelphia, PA 19122, USA*
[b] *Department of Chemical Engineering, University of Pittsburgh, Pittsburgh, PA 15261, USA*
[c] *Department of Chemistry and Institute for Advanced Research, Nagoya University, Nagoya 464-8602, Japan*
[d] *Departement of Civil and Environmental Engineering, University of Pittsburgh, Pittsburgh, PA 15261, USA*

ARTICLE INFO

Article history:
Received 24 December 2008
Accepted 9 November 2009
Available online 17 November 2009

ABSTRACT

The interaction of acetone with single wall carbon nanotubes (SWCNTs) was studied by temperature programmed desorption with mass spectrometry (TPD-MS), after reflux, sonication, or exposure to 7.6 Torr of acetone vapors at room temperature. Acetone molecules adsorb strongly on SWCNTs desorbing at ~400–900 K, corresponding to desorption energies of ~100–225 kJ/mol, as intact molecules. Exchange of intact adsorbed molecules with gas phase species was observed in successive dosing of hydrogenated and deuterated acetone molecules. The desorption energies reported here are in stark contrast to the desorption energies (~75 kJ/mol) reported earlier for SWCNTs interacting with acetone under high vacuum at cryogenic temperatures. This result suggests activated adsorption/desorption, and is also observed for adsorption of ethanol, methane, *n*-butane and 1,3-butadiene on SWCNTs and on carbon black. Quantum chemical calculations suggest that adsorption in interstitial channels of bundles formed of large-diameter SWCNTs is possible and can account for high desorption barriers, a result of strong dispersion interactions between neighboring SWCNTs.

1. Introduction

The interaction of carbon nanotubes (CNTs) with solvents is important for applications of CNTs in nanofluidic devices [1,2], the development of CNT based sensors [3–6], and the technological processing of CNTs [7,8]. It is important to know the influence of different conditions on the interaction of CNTs with solvents. The dispersion of CNTs in solvents often involves sonication, a process that is accompanied by changes in temperature and pressure that can favor chemical reactions that would not proceed under normal conditions [7,9,10].

There is ongoing interest in acetone interaction with CNTs for sensor applications [3–6,11]. Acetone is used as a solvent to prepare CNTs-polymer composites [8]. However, there is no general agreement on the nature of the interaction of acetone with nanotubes. Recently, Chakrapani et al. reported that SWCNTs, sonicated in acetone, interact with acetone chemically [12]. Shih and Li also suggested that acetone vapor interacts chemically with multiwall carbon nanotubes

* *Corresponding author:* Address: Department of Chemistry, Temple University, Philadelphia, PA 19122, USA. Fax: +1 215 204 9530.
E-mail address: eborguet@temple.edu (E. Borguet).
0008-6223/$ - see front matter © 2009 Elsevier Ltd. All rights reserved.
doi:10.1016/j.carbon.2009.11.018

(MWCNTs) in the temperature range 303–363 K [13]. Kazachkin et al., studying cryogenic (100 K) acetone adsorption on SWCNTs, found no evidence for a chemical interaction and concluded that acetone adsorbs reversibly on SWCNTs [14]. The different conditions used may be the reason for the range of different observations reported [12–14].

The present paper reports a study of the interaction of acetone with SWCNTs upon reflux, sonication, and exposure to solvent vapors. The initial objective of the present work was to find out whether different treatment conditions (e.g., reflux, sonication) of SWCNTs in solvents may result in chemical interaction between solvents and SWCNTs. In the course of the study it was found that even after exposure of SWCNTs to acetone vapors at ambient conditions acetone can strongly[1] adsorb on SWCNTs, desorbing upon heating as intact molecules at ~400–900 K with desorption energies ~100–225 kJ/mol. In contrast, strong adsorption does not take place when acetone is exposed to SWCNTs at cryogenic temperatures and high vacuum conditions [14].

2. Experimental

2.1. Materials

As-produced SWCNTs, synthesized by the HiPco [15] method, were air/HCl purified according to the procedure described in [14]. The iron content was ~20 wt.% for as-produced SWCNTs and ~1 wt.% after air/HCl purification [14]. Specific surface area for as-produced SWCNTs was 625 m^2/g and 50% of the pores had a diameter less than 2 nm with maximum at 1.3 nm (see Fig. S1 in Supporting Information).

Carbon black (CB-460, Cabot) was used as a model compound to mimic carbonaceous impurities present in as-produced CNTs. Carbon black is produced by incomplete combustion of organics [16] and characterized by limited porous structure [17]. Carbon black used in this work had a specific surface area of ~76 m^2/g and 95% of the pores were larger than 5 nm (Fig. S1).

2.2. Sample preparation

Carbon materials were treated in acetone under different conditions (reflux, sonication or exposure to acetone vapors) to find out how the treatment influences the interaction of acetone with SWCNTs. The air/HCl purified SWCNTs were either refluxed or sonicated in acetone before loading into the vacuum chamber. For sonication, ~0.5–1 mg of the SWCNTs was treated in ~3 ml of solvent for 3 h using a laboratory ultrasonic cleaner (Branson, 2510R). For reflux, ~0.5–1 mg of SWCNTs were boiled in ~3 ml of solvent for 3 h. After pre-treatment the sample was deposited at ambient temperature by drop-and-dry method onto a W-grid (AlfaAesar, 0.002") connected to the sample holder. A fast response K-type thermocouple (Omega) was spot-welded to the W-grid before sample deposition. The design of the sample holder allows sample cooling to ~100 K and controlled heating to 1400 K [18]. After deposition onto the W-grid, the sample was placed in a TPD vacuum chamber and evacuated overnight to $< 10^{-8}$ Torr[2]. Before TPD-MS experiments, the sample was cooled to ~100 K.

Acetone-d6 ($(CD_3)_2CO$, Acros, 99.5% D) was used as received. Ultra-pure water, used to sonicate SWCNTs in a control experiment, was produced by a water purification system (Easypure II UV, Barnstead). Samples sonicated in water did not have any contact with acetone and TPD-MS results obtained from those samples were used as a control. For *in situ* experiments, when acetone vapors were dosed to samples in the ultrahigh vacuum chamber, liquid acetone was degassed by 4–7 freeze–pump–thaw cycles. The purity of degassed acetone was verified with MS.

2.3. TPD-MS measurements

The TPD-MS studies were performed to address the nature of species desorbing from carbon materials before and after different treatments in acetone. The studies were conducted in a stainless steel ultrahigh vacuum chamber equipped with residual gas analyzer RGA 300 (SRS, CA) [18]. The base pressure in the vacuum chamber before experiments was $<10^{-8}$ Torr. Initially the sample was cooled to ~100 K with liquid nitrogen and then heated at 2 K/s to the desired temperature (>900 K) with simultaneous monitoring of all the MS-fragments desorbing in the 1–70 amu range. Typical resolution for the TPD-MS spectrum was 1 data point for a given mass per 8 K.

The interaction of acetone vapors with SWCNTs and carbon black was investigated at 300 K to understand the effects of sonication or reflux. For that purpose SWCNTs or carbon black vacuum-annealed at 900 K (0.5 h) was exposed to 7.6 Torr of solvent vapors at 300 K for 10 min inside the TPD chamber. After exposure the TPD chamber was evacuated for 20 h at 300 K to $<10^{-8}$ Torr. Then the sample was cooled to ~100 K and the TPD spectrum was collected.

Acetone adsorption experiments at 100 K were performed according to the procedure described in [14]. For that purpose, acetone vapors were dosed to a sample vacuum-annealed at 900 K (0.5 h) and then cooled to 100 K. After dosing a TPD-MS spectrum (1–70 amu) was recorded. The objective of the low temperature adsorption experiment was to estimate the amount of acetone retained by samples after sonication, reflux, or exposure to 7.6 Torr of solvent vapors, i.e. to determine the dose (in Langmuir equivalent) needed to obtain the same MS signal intensity.

3. Results and discussion

3.1. Interaction of acetone with SWCNTs

Acetone-d6 was selected for the study to facilitate the MS-analysis, in particular to distinguish peaks due to acetone and those "intrinsic" to the SWCNTs. Upon heating both the as-produced and air/HCl purified SWCNTs that had no con-

[1] The term "strongly interact" will be used here to characterize molecular desorption with energies > 100 kJ/mol.

[2] We use the units of Torr for pressure (1 Torr = 133 Pa) and Langmuir for exposure (1 L = 10^{-6} Torr * sec). The conversion between pressure units is given in Table S1 of Supporting Information.

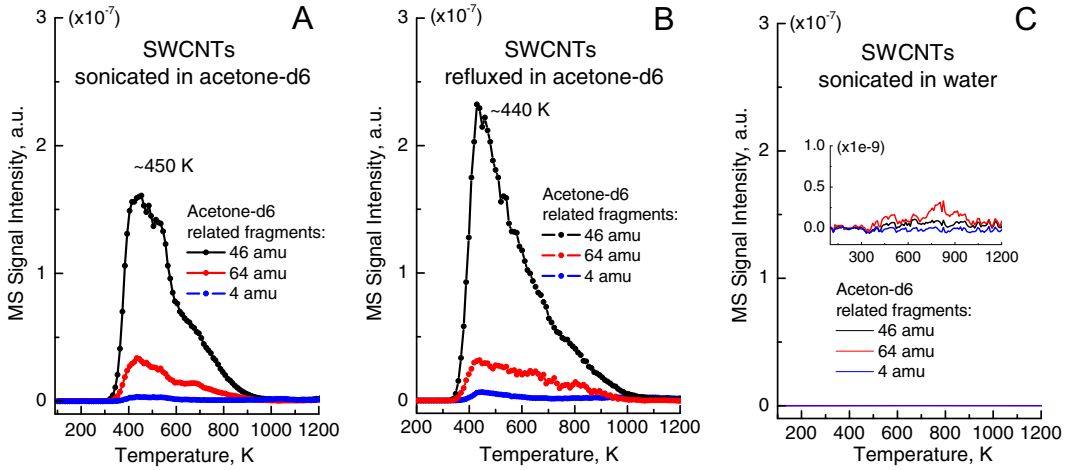

Fig. 1 – TPD profiles of acetone-d6 MS-fragments evolving from purified SWCNTs (A) sonicated in acetone-d6; (B) refluxed in acetone-d6; (C) sonicated in ultra-pure water. SWCNTs treated in acetone-d6 release ~100 times more acetone-d6 related MS-fragments than SWCNTs sonicated in water.

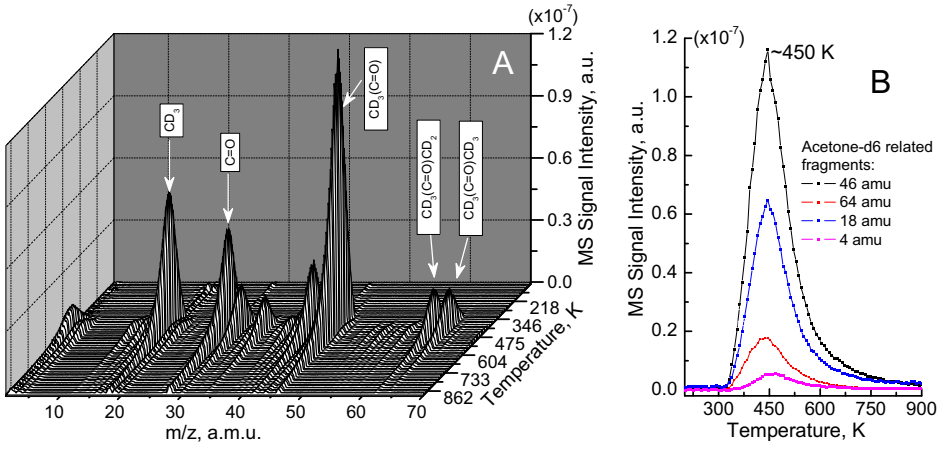

Fig. 2 – Comparison of TPD profile of acetone-d6 (46 amu – CD_3CO) adsorbed at ~10^{-6} Torr–100 K (blue curve) to profile of acetone adsorbed at 7.6 Torr–300 K (black curve). (A) TPD spectrum collected from purified SWCNTs, vacuum-annealed (900 K, 0.5 h), and exposed to 7.6 Torr of acetone-d6 (300 K, 10 min); (B) selected acetone-d6 fragments extracted from the TPD spectrum are plotted versus temperature. Exposure of SWCNTs to acetone vapors results in as strong acetone adsorption on SWCNTs as after reflux or sonication (Fig. 1A and B). (For interpretation of the references to color in this figure legend, the reader is reffered to the web version of this article.)

tact with acetone released multiple MS-fragments that can be misinterpreted as fragments of acetone-h6 and/or acetone-d6 (Figs. S2 and S3). However, the relative intensity of MS-fragments that can be assigned to acetone-d6 was approximately 10 times less than the intensity of MS-fragments that can be assigned to acetone-h6 (Fig. S3). However, to provide better contrast acetone-d6 was selected for the study. The fragments 4 amu (D_2), 46 amu (CD_3CO) and 64 amu ($CD_3C(=O)CD_3$) had negligible intensity in TPD spectra of SWCNTs not exposed to acetone (Fig. 1C) and consequently were chosen to characterize acetone-d6 desorption without interference from fragments "intrinsic" to SWCNT samples.

Purified SWCNTs sonicated (Fig. 1A) or refluxed (Fig. 1B) in acetone-d6 revealed ~100 times more intense TPD-MS signals corresponding to acetone-d6 fragments than purified SWCNTs that had no contact with acetone-d6 (Fig. 1C). The similarity in intensity of acetone-d6 fragments from SWCNTs refluxed or sonicated in acetone-d6 (Fig. 1A and B), within the reproducibility of the measurements (Fig. S4), suggests that the amount of acetone that adsorbs on SWCNTs is not significantly affected by the treatment procedure (reflux or sonication).

To elucidate the role of reflux and sonication on the interaction of acetone with SWCNTs, the adsorption of acetone vapors was investigated. On the first day, 7.6 Torr of acetone-d6 vapors were exposed (300 K, 10 min) to SWCNTs that had previously been vacuum-annealed at 900 K for 0.5 h. Then the TPD chamber was evacuated overnight. On the next day, a TPD experiment revealed that acetone-d6 adsorbed from the gas phase interacts with SWCNTs in a similar way as after

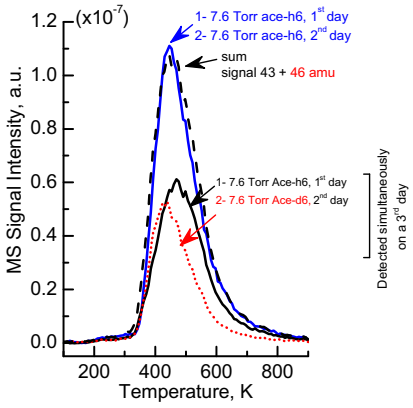

Fig. 3 – Gas phase exchange experiment. SWCNTs with pre-adsorbed acetone-h6 were exposed to acetone-d6 and after evacuation MS-fragments of acetone-h6 and acetone-d6 were collected simultaneously. Pre-adsorbed acetone-h6 can be partially replaced with acetone-d6.

reflux or sonication, desorbing upon heating with a maximum at ~450 K (Fig. 2B), but without the high temperature tails (800–1000 K) observed in Fig. 1A and B.

Acetone-d6 related MS-fragments desorbing from SWCNTs either after sonication, reflux, or dosing from the gas phase have similar temperature profiles (Fig. S5). The relative intensity of signals for the different fragments is similar to intensities of those fragments for acetone-d6 in the gas phase, suggesting that acetone retained by SWCNTs desorbs upon heating as intact molecules.

To further test the hypothesis of molecular adsorption/desorption of acetone on/from SWCNTs, an experiment was performed to find out if acetone adsorbed on SWCNTs can be replaced (exchanged) with acetone from the gas phase. To start, SWCNTs annealed to 900 K were exposed to 7.6 Torr of acetone-h6 ($(CH_3)_2CO$) inside a TPD chamber for 10 min at 300 K after which the sample was evacuated overnight to $<10^{-8}$ Torr. On the next day, the sample was exposed to 7.6 Torr of acetone-d6 ($(CD_3)_2CO$) for 10 min at 300 K. After overnight evacuation to $<10^{-8}$ Torr the sample was cooled to 100 K and a TPD spectrum was collected (Fig. 3). A control experiment, involving acetone-h6 dosing on two successive days followed by TPD, was also performed. The sum (black dashed curve) of signals from first acetone-h6 (black solid curve) and acetone-d6 (red dotted curve)[3] is equal the signal from acetone-h6 (blue curve) after two doses of acetone-h6 suggesting that all available sites are saturated with acetone and that the second dose does not add any additional acetone molecules (Fig. 3). The results of these experiments suggest that acetone desorbing from SWCNTs with high energies (>100 kJ/mol) can exchange with acetone from the gas phase (Fig. 3). Analysis of intensities and temperature desorption profiles of different fragments of acetone-h6 and -d6 showed that both molecules desorb intact.

The amount of acetone desorbing from SWCNTs after sonication and reflux (Fig. 1A and B) is comparable to the amount of acetone desorbing after exposure of SWCNTs to acetone vapors (Fig. 1A and B) suggesting that most of the sites with high desorption energy are saturated already after first exposure of SWCNTs to 7.6 Torr of acetone vapors. From Fig. 3 it follows that acetone pre-adsorbed on SWCNTs can be partially replaced by acetone from the gas phase. Notice that the maximum peak position of acetone-d6 (adsorbed on "top" of acetone-h6) after the exchange experiment was at 425 K while the peak maximum of acetone-h6 was at 470 K (Fig. 3); acetone-d6 that was dosed to the sample with pre-adsorbed acetone-h6 replaced preferentially acetone-h6 molecules that had lower desorption energies. The estimated exchange probability of acetone-h6 to acetone-d6 was estimated to be $\sim 10^{-7}$ (Section VIII of Supporting Information). Acetone desorbing from SWCNTs with high energies (>100 kJ/mol) can exchange with acetone from the gas phase suggesting that adsorbed acetone preserves its molecular structure.

According to the results of the present work acetone preserves its chemical structure when adsorbed on SWCNTs even after sonication and reflux procedures (Fig. 1). This finding contradicts previous reports for SWCNTs [12] and MWCNTs [13]. The absence of correlation in TPD profiles of different acetone related fragments observed in [12] can originate from desorption of organics adsorbed from ambient air (Figs. S2 and S3). No control experiments were reported for SWCNTs that were not treated with acetone [12]. The conclusion regarding chemical reaction between MWCNTs and acetone was based on the observed desorption energy for acetone (~68 kJ/mol) and no additional experimental analysis was provided [13].

The interaction of acetone with carbon black, used as a model to simulate possible carbonaceous impurities in SWCNTs, was investigated. When acetone is adsorbed at cryogenic temperature on carbon black desorption peaks similar to acetone desorption from SWCNTs were reported [14]. Carbon black annealed under vacuum at 900 K for 0.5 h and then exposed to 7.6 Torr of acetone (300 K, 10 min) revealed desorption of acetone fragments (Fig. 4A) with similar TPD profiles suggesting molecular acetone desorption (not shown).

One of the intriguing observations reported here is the difference in binding energy after dosing molecules at ambient conditions (7.6 Torr, 300 K) and at cryogenic temperatures under high vacuum (10^{-6} Torr, 100 K) [14]. Exposure of the samples to "low pressures" (10^{-6} Torr) and temperatures (100 K) does not allow access to sites with high desorption temperatures (~450 K) (Fig. 4, Figs. S7 and S8) [14,19]. The limited access to the sites with high desorption energies for molecules dosed at 10^{-6} Torr–100 K can be explained by activated adsorption. The concept of activated adsorption was introduced by Taylor in 1931 [20] and can be represented by Fig. 5.

In the case of adsorption at cryogenic temperatures under high vacuum (10^{-6} Torr, 100 K), where the number of adsorption events is determined by exposure, sites with no or small activation energy are easily filled. In the case of higher tem-

[3] For interpretation of the references to color in this figure, the reader is referred to the web version of this article.

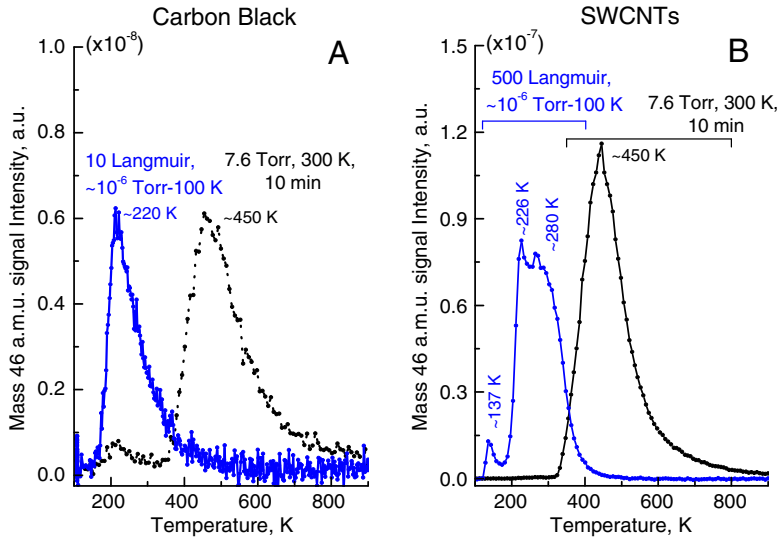

Fig. 4 – Comparison of TPD profile of acetone-d6 (46 amu – CD_3CO) adsorbed at ~10^{-6} Torr–100 K (blue curve) to profile of acetone adsorbed at 7.6 Torr–300 K (black curve). (A) Adsorption of acetone on carbon black annealed to 900 K (0.5 h); (B) adsorption of acetone on the purified SWCNTs annealed to 900 K (0.5 h). The TPD analysis was performed immediately after 100 K–10^{-6} Torr dosing and reducing pressure to $\leqslant 10^{-8}$ Torr (5 min evacuation after dosing). In turn, after 300 K–7.6 Torr dosing the samples were evacuated for 20 h at 300 K to reduce background pressure to $<10^{-8}$ Torr. (For interpretation of the references to color in this figure legend, the reader is referred to the web version of this article.)

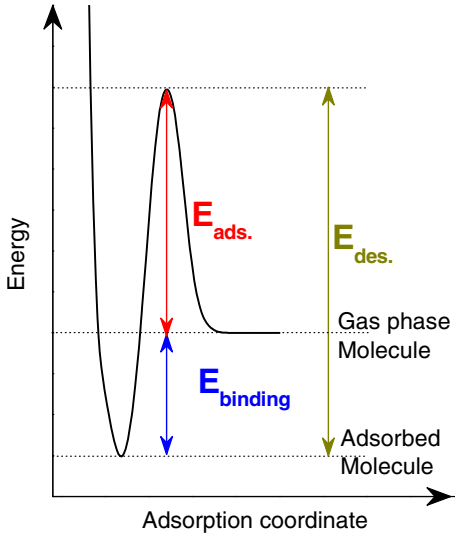

Fig. 5 – Potential energy profile for activated adsorption.

perature (300 vs. 100 K) and pressure (7.6 vs. 10^{-6} Torr) dosing, the probability of overcoming the activation barrier becomes higher due to increased number of collisions with the surface (see Section VIII of Supporting Information). It appears that experimental techniques utilizing the adsorption of gases (solvent vapors) under low pressures and temperatures do not allow probing all of available sites in porous carbons due to the adsorption/desorption pressure gap effect revealed in this work.

The adsorption capacity with respect to acetone of the air/HCl purified SWCNTs exceeds the adsorption capacity of carbon black by at least 50 times (Fig. 4). The adsorption capacity of carbon materials depends on the availability of micropores. Carbon nanotubes can retain at least 50 times more strongly adsorbed acetone than carbon black. Carbon black has a surface area of ~74 m^2/g and macro-porous structure (most of the pores > 5 nm) (Fig. S1). In turn, SWCNTs have surface area ~625 m^2/g (Fig. S1) and large fraction of the micropores is defined by the nanotube diameter (~1–2 nm) [21–23]. If the amount of acetone adsorbed is proportional to the surface area, then the difference in the uptake capacity between carbon black and SWCNTs should be at most ~10 times. We believe that the uptake capacity of carbonaceous materials studied here is defined by their microporous structure and the observed adsorption/desorption behavior is due to activated processes for molecules to enter/leave narrow pores in porous carbon materials.[4] Similar results were obtained for ethanol (Fig. S7), *n*-butane, and 1,3-butadiene (Fig. S8) exposed to SWCNTs in the same way as acetone, suggesting that other molecules can also strongly adsorb on SWCNTs and desorb molecularly at 400–800 K.

3.2. *Quantum chemical modeling of acetone adsorption on individual SWCNTs and SWCNT bundles*

The characterization of the nature of adsorption sites, corresponding to the experimentally observed desorption energies was set as the objective for theoretical investigations. Previously, we computed the binding energies for acetone

[4] We relate the amount of acetone strongly bound to SWCNTs after 7.6 Torr–300 K to the amount of acetone adsorbed by the same sample at 10^{-6} Torr–100 K. In such cases the mass of the sample deposited should not influence the amount of acetone bound under different T–P conditions. Instead the specific properties of the sample (surface area, porosity, etc.) will define the adsorption capacity.

adsorbed inside and outside small (6,5) and large (11,9) diameter SWCNTs [14], using dispersion augmented self-consistent-charge density-functional tight-binding (DFTB-D) [24,25] after benchmarking this method against counterpoise-corrected large basis set MP2 calculations for the acetone-coronene model system [14]. Binding energies ($E_{binding}$ defined here as $E_{complex} - E_{sorbent} - E_{adsorbate}$ = interaction energies between sorbent and adsorbate species) were found to depend strongly on the sidewall curvature in the case of endohedral absorption, while exohedral adsorption displays a less pronounced dependence [14]. Endohedral adsorption inside small-diameter tubes is strongest with $E_{binding}$ = −74.4 kJ/mol for the (6,5) tube, and weakest for exohedral adsorption with $E_{binding}$ = −26.3 kJ/mol (11,9) and $E_{binding}$ = −24.6 kJ/mol (6,5) for the energetically most favorable planar parallel conformation of acetone [14]. The desorption energies in excess of 100 kJ/mol observed in this work for molecularly desorbing species (Fig. 1) call for an alternative explanation.

3.2.1. *Acetone adsorbed on SWCNT sidewall defects*

Acetone binding energies with Stone–Wales and mono-vacancy defect sites were computed using hydrogen-terminated, 10 Å-long tube fragments of a large- (11,9) (L) and a small-diameter (6,5) (S) [14]. Stone–Wales defects increase the magnitude of ΔE of the weaker exohedral adsorption only by 6 to ~20 kJ/mol, while endohedral adsorption is less affected (differences with pristine SWCNT systems are smaller than 6 kJ/mol). We chose 5/9-type defects to model a mono-vacancy defect [26]. Endohedral adsorption inside a mono-vacancy defect containing (6,5) SWCNT bears a binding energy of −78.4 kJ/mol. Neither Stone–Wales nor mono-vacancy defects can cause increase in binding energies to >100 kJ/mol.

3.2.2. *Acetone adsorbed in groove sites*

We calculated binding energies for acetone in grooves formed by large- (L) and small-diameter (S) nanotubes: LL, LS, and SS (Fig. 6). Table 1 lists the interaction energies $\Delta E_{SWCNT-SWCNT'} = E_{groove} - E_{SWCNT} - E_{SWCNT'}$ between nanotubes with no acetone adsorbed. The interaction energy between tubes becomes larger in magnitude with the diameter of the constituent tubes (Table 1). The DFTB-D result of −155.9 kJ/mol seems to be very reasonable for the interaction between two 10 Å-long (11,9) SWCNTs (Table 1) in the view of results published in Reference [27].

Energies for acetone placed in the groove site (LacL, LacS, or SacS) were calculated (Table 1). We find a narrow range of total DFTB-D binding energies of acetone with the tube dimers from 46 to 48 kJ/mol (Table 1), which is roughly 1.9 times the value of exohedral adsorption on a single tube [14]. Clearly, groove sites can not be responsible for the desorption energies (>100 kJ/mol) observed experimentally.

3.2.3. *Acetone adsorbed in interstitial sites*

Due to the narrow space, interstitial sites of perfectly aligned SWCNTs in bundles are generally not accessible for adsorbate molecules [28]. However, theoretical simulations predict that for bundles formed of carbon nanotubes of different diameter the interstitial sites can be accessed by such molecules as Ar, CH_4, and Xe [29,30]. We attempted to compute optimized geometries for acetone adsorbed inside interstitial sites of the four different bundles comprised of L and S tubes: LLL, LLS, LSS, and SSS. We found local minima for acetone only inside LLL and LLS bundles, while corresponding structures for LSS and SSS disintegrated during geometry optimization. The total binding energy of −54.0 kJ/mol for acetone in the interstitial site of the LLL bundle is close to adsorption in groove sites (Table 1), but smaller on a per-tube basis (3 tubes vs. 2). The tubes undergo significant deformation in the presence of acetone with a deformation energy (DEF) of 16.7 kJ/mol relative to the geometry of the LLL bundle without acetone, while the interaction energy (INT) with the deformed tubes is −70.7 kJ/mol ($E_{binding}$ = DEF + INT). Nevertheless, acetone physisorption inside the interstitial channel of an all-large diameter tube LLL bundle seems energetically feasible. The deformation of the tubes in the presence of the acetone is shown for the LLS system in Fig. 7. Here, the binding energy $E_{binding}$ becomes positive 2.2 kJ/mol and corresponding values for DEF and INT are 82.4 and −80.2 kJ/mol, respectively.

The following example can explain the observed adsorption/desorption pressure gap effect that can originate from

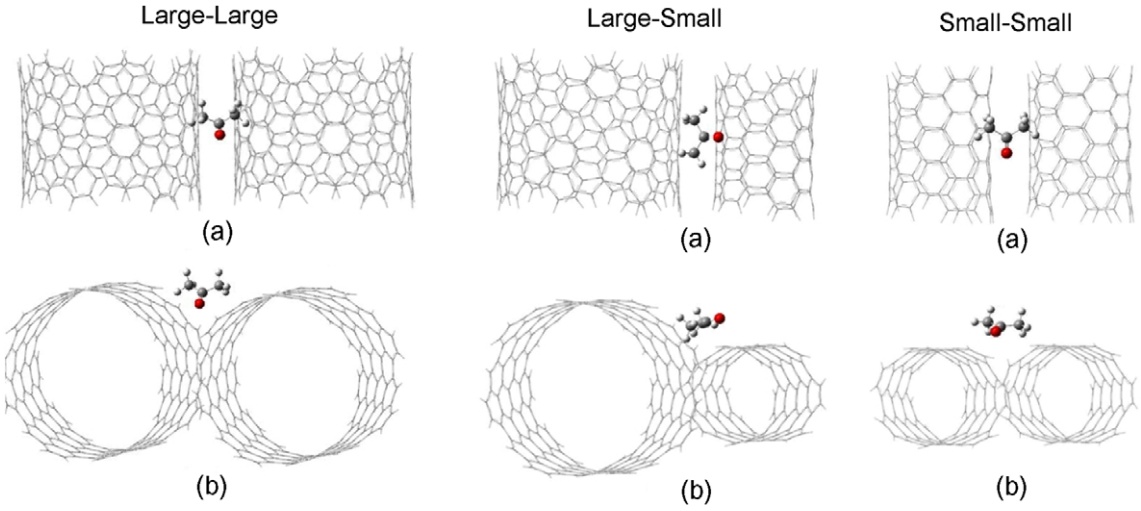

Fig. 6 – Representative optimized geometries for acetone adsorbed in LL, LS, and SS groove sites. (a) Top view and (b) skewed front view.

Table 1 – Interaction energies $\Delta E_{SWCNT-SWCNT'}$ (kJ/mol) for dimers of 10 Å-long, hydrogen-terminated (11,9) (L) and (6,5) (S) tube fragments, and for acetone in the groove sites of tube dimers, averaged over six optimized geometries of acetone orientation. Energy contributions are listed as follows: total $\Delta E_{SWCNT-SWCNT'}$ (DFTB-D), which is the sum of DFTB-only contribution and dispersion energy contribution (D-only).

Compound	DFTB-D	DFTB-only	D-only
SWCNT–SWCNT			
LL	−155.89	5.73	−161.61
LS	−125.57	11.53	−137.10
SS	−105.39	3.12	−108.51
SWCNT–acetone–SWCNT (average)			
LacL	−48.16	12.88	−61.04
LacS	−46.08	0.89	−46.98
SacS	−47.25	5.77	−53.01

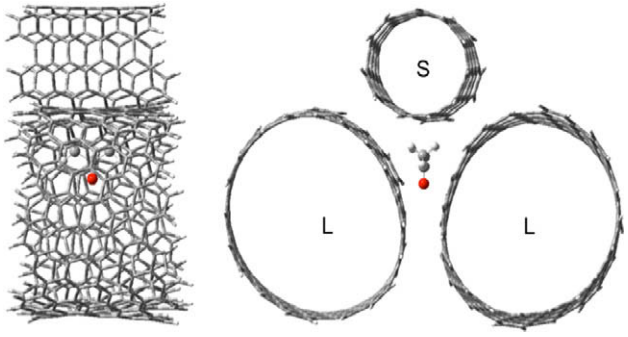

Fig. 7 – Optimized geometry for acetone adsorbed inside the interstitial site of an LLS bundle.

activated adsorption on sites that have physical limitations for access, e.g., interstitial channels. SWCNT bundles may have interstitial channels that are not accessible to gas molecules greater than a certain size (acetone, butane, etc.). When such molecules approach the SWCNT bundles, they may occasionally squeeze into interstitial channels and "debundle" nanotubes while moving along interstitial channels and filling them (Fig. 8). Molecules that are close to the exit of interstitial channels may desorb first, while molecules that are far away from the interstitial channel exit may be "trapped", because physisorption to the SWCNT sidewalls decreases their mobility. The energies $\Delta E_{SWCNT-SWCNT'}$ that hold SWCNTs in bundles are of van der Waals nature [27] and our calculations suggest that SWCNTs can interact with energy of ~150 kJ/mol for every nanometer of interaction length (Table 1). This is a rough estimate for the energy that one would need to supply to move SWCNTs apart from each other and create an "exit" for molecules to escape from interstitial channel ($\Delta E_{SWCNT-SWCNT'}$ corresponds to the barrier $E_{ads.}$ in Fig. 5). The molecules that are squeezed between SWCNTs inside the interstitial channel need to overcome the energy of the interaction between SWCNTs to diffuse along the interstitial channel. In general, narrow pores (pores whose size is similar to adsorbate dimensions) in carbon materials can require activation energy for adsorbates to diffuse along them.

To conclude, the observed desorption energies $E_{des.}$ may originate in desorption of molecules from interstitial sites of nanotube bundles (Fig. 8). The interaction energies $\Delta E_{SWCNT-SWCNT'}$ between nanotubes are ~100–160 kJ/(mol nm) (Table 1) and an increase in the distance between two tubes causes a rapid decrease, of $\Delta E_{SWCNT-SWCNT}$ due to the r^{-6} dependence of the dispersion energy. Thus, desorption of molecules from the interstitial sites can be associated with energy barriers

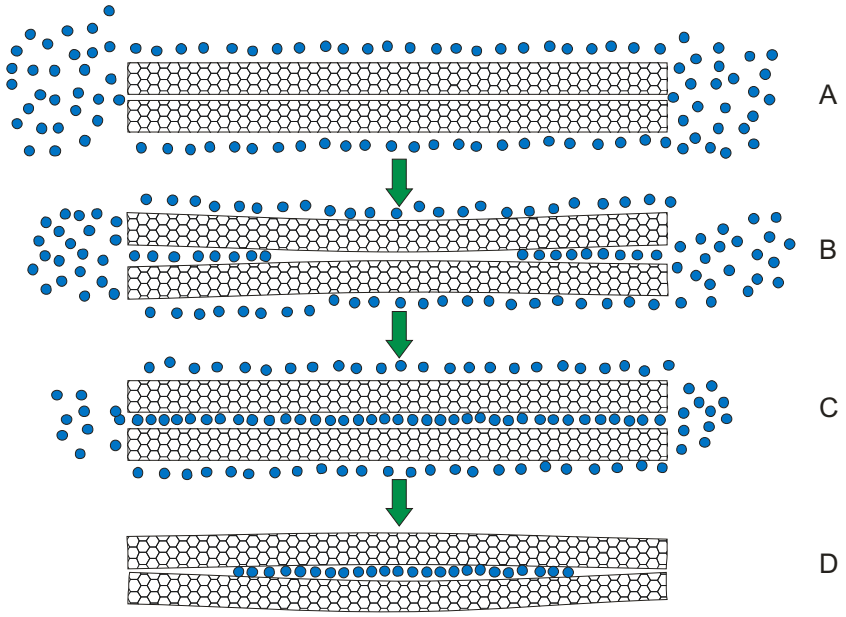

Fig. 8 – Proposed model describing activated adsorption/desorption mechanism of molecules inside interstitial channels of a SWCNT bundle. Molecules approach the SWCNT bundle (side view shows only two nanotubes for simplicity) (A) and start to penetrate the interstitial channel "debundling" nanotubes (B). Ultimately molecules fill the whole interstitial channel (C). Upon evacuation molecules that are close to the "exits" will desorb first, while molecules that are in the middle of interstitial channels can be trapped inside (D). Elastic deformation of carbon nanotubes may assist trapping of the molecules (D).

$E_{ads.} = \Delta E_{SWCNT-SWCNT'}$ easily in excess of 100 kJ/mol which are required to open up an "exit channel" between the tubes, for instance >156 kJ/(mol nm) in case of L-bundles. Other possibilities for causing adsorption barriers E_{ads} include small-size SWCNT sidewall holes that block passage of molecules entering or leaving the SWCNT interior space.

It should be pointed out that while the temperature desorption profiles for acetone interacting with SWCNTs are very similar for different pretreatments (reflux, sonication, or exposure to acetone vapors), samples that were sonicated and refluxed in acetone revealed long temperature tale up to 900-1000 K (Fig. 2). Even in that temperature range acetone desorbs as an intact molecule; different MS-fragments of acetone coincide (Fig. S5). It is clear that aggressive conditions such as sonication and/or reflux enable acetone to access adsorption sites of SWCNT bundles that adsorption under cryogenic conditions cannot reach.

4. Summary

Acetone molecules (and other simple organic molecules (see Supporting Information)) at near ambient pressure and temperature can appear to be strongly adsorbed on SWCNTs desorbing at ~400–900 K (corresponding to binding energies ~100–225 kJ/mol) under high vacuum. The observed desorption energies are much higher than those reported for similar molecules adsorbed under high vacuum at cryogenic temperatures. Even when molecules appear strongly adsorbed, the molecules studied here desorb as intact species. The appearance of strong adsorption at near ambient pressure and temperature was found to be caused by barriers for adsorption and desorption as shown in Fig. 5, adding to the binding energies of the molecules with the SWCNTs.

The findings presented here have a number of implications. The developers of CNT based sensors, especially for organic molecule detection [3,4,6,31], should be aware of strong adsorption of those molecules to carbon nanotubes; strongly adsorbed molecules can deteriorate the performance of CNT based sensors. Control experiments revealed that SWCNTs, upon heating in vacuum, release organics that presumably were adsorbed from ambient air (Figs. S2 and S3). The adsorption of most organic molecules investigated here is "irreversible" at room temperature as temperatures >450–490 K are needed to remove the adsorbed gases in a reasonable amount of time. In order to keep SWCNTs "clean" it is advised to heat them to >600–650 K when most of the molecules studied here desorb. Such temperatures are reasonable for purified SWCNTs that typically do not start to burn up to ~700 K in air [14,32].

Acknowledgements

SI acknowledges support by the Program for Improvement of Research Environment for Young Researchers from the Ministry of Education, Culture, Sports, Science and Technology (MEXT) of Japan and by a special grant from JSPS in Priority Area "Molecular Theory for Real Systems". EB and DK acknowledge the support of US DOE Office of Basic Energy Sciences.

Appendix A. Supplementary data

Supplementary data associated with this article can be found, in the online version, at doi:10.1016/j.carbon.2009.11.018.

REFERENCES

[1] Noy A, Park HG, Fornasiero F, Holt JK, Grigoropoulos CP, Bakajin O. Nanofluidics in carbon nanotubes. Nano Today 2007;2(6):22–9.
[2] Holt JK, Park HG, Wang Y, Stadermann M, Artyukhin AB, Grigoropoulos CP, et al. Fast mass transport through sub-2-nanometer carbon nanotubes. Science 2006;312(5776):1034–7.
[3] Robinson JA, Snow ES, Badescu SC, Reinecke TL, Perkins FK. Role of defects in single-walled carbon nanotube chemical sensors. Nano Lett 2006;6(8):1747–51.
[4] Snow ES, Perkins FK. Capacitance and conductance of single-walled carbon nanotubes in the presence of chemical vapors. Nano Lett 2005;5(12):2414–7.
[5] Guirado-Lopez RA, Sanchez M, Rincon ME. Interaction of acetone molecules with carbon-nanotube-supported TiO_2 nanoparticles: possible applications as room temperature molecular sensitive coatings. J Phys Chem C 2007;111(1):57–65.
[6] Parikh K, Cattanach K, Rao R, Suh D-S, Wu A, Manohar SK. Flexible vapour sensors using single walled carbon nanotubes. Sens Actuators B Chem 2006;B113(1):55–63.
[7] Koshio A, Yudasaka M, Zhang M, Iijima S. A simple way to chemically react single-wall carbon nanotubes with organic materials using ultrasonication. Nano Lett 2001;1(7):361–3.
[8] Owens FJ, Jayakody JRP, Greenbaum SG. Characterization of single walled carbon nanotube: polyvinylene difluoride composites. Compos Sci Technol 2006;66(10):1280–4.
[9] Suslick KS. Sonochemistry. Science 1990;247(4949, Pt. 1):1439–45.
[10] Huang WJ, Lin Y, Taylor S, Gaillard J, Rao AM, Sun YP. Sonication-assisted functionalization and solubilization of carbon nanotubes. Nano Lett 2002;2(3):231–4.
[11] Lu Y, Partridge C, Meyyappan M, Li J. A carbon nanotube sensor array for sensitive gas discrimination using principal component analysis. J. Electroanal Chem 2006;593(1–2):105–10.
[12] Chakrapani N, Zhang YM, Nayak SK, Moore JA, Carroll DL, Choi YY, et al. Chemisorption of acetone on carbon nanotubes. J Phys Chem B 2003;107(35):9308–11.
[13] Shih Y-h, Li M-s. Adsorption of selected volatile organic vapors on multiwall carbon nanotubes. J Hazard Mater 2008;154(1–3):21–8.
[14] Kazachkin D, Nishimura Y, Irle S, Morokuma K, Vidic RD, Borguet E. Interaction of acetone with single wall carbon nanotubes at cryogenic temperatures: a combined temperature programmed desorption and theoretical study. Langmuir 2008;24(15):7848–56.
[15] Nikolaev P, Bronikowski MJ, Bradley RK, Rohmund F, Colbert DT, Smith KA, et al. Gas-phase catalytic growth of single-walled carbon nanotubes from carbon monoxide. Chem Phys Lett 1999;313(1–2):91–7.
[16] Donnet JB, Bansai RC, Wang MJ, editors. Carbon black: science and technology. 2nd ed.; 1993.
[17] Bradley RH, Sutherland I, Sheng E. Carbon surface: area, porosity, chemistry, and energy. J Colloid Interface Sci 1996;179(2):561–9.
[18] Kwon S, Borguet E, Vidic RD. Impact of surface heterogeneity on mercury uptake by carbonaceous sorbents under UHV and

atmospheric pressure. Environ Sci Technol 2002;36(19):4162–9.
[19] Ulbricht H, Zacharia R, Cindir N, Hertel T. Thermal desorption of gases and solvents from graphite and carbon nanotube surfaces. Carbon 2006;44(14):2931–42.
[20] Taylor HS. The activation energy of adsorption processes. J Am Chem Soc 1931;53(2):578–97.
[21] Yang CM, Kanoh H, Kaneko K, Yudasaka M, Iijima S. Adsorption behaviors of HiPco single-walled carbon nanotube aggregates for alcohol vapors. J Phys Chem B 2002;106(35):8994–9.
[22] Yang CM, Kaneko K, Yudasaka M, Iijima S. Effect of purification on pore structure of HiPco single-walled carbon nanotube aggregates. Nano Lett 2002;2(4):385–8.
[23] Cinke M, Li J, Chen B, Cassell A, Delzeit L, Han J, et al. Pore structure of raw and purified HiPco single-walled carbon nanotubes. Chem Phys Lett 2002;365(1–2):69–74.
[24] Elstner M, Hobza P, Frauenheim T, Suhai S, Kaxiras E. Hydrogen bonding and stacking interactions of nucleic acid base pairs: a density-functional-theory based treatment. J Chem Phys 2001;114:5149–55.
[25] Elstner M, Porezag D, Jungnickel G, Elsner J, Haugk M, Frauenheim T, et al. Self-consistent-charge density-functional tight-binding method for simulations of complex materials properties. Phys Rev B 1998;58:7260–8.
[26] Hashimoto A, Suenaga K, Gloter A, Urita K, Iijima S. Direct evidence for atomic defects in graphene layers. Nature 2004;430(7002):870–3.
[27] Szabados A, Biro LP, Surjan PR. Intertube interactions in carbon nanotube bundles. Phys Rev B Condens Matter Mater Phys 2006;73(19):195404–9.
[28] Kondratyuk P, Yates J. Molecular views of physical adsorption inside and outside of single-wall carbon nanotubes. Acc Chem Res 2007;40(10):995–1004.
[29] Shi W, Johnson JK. Gas adsorption on heterogeneous single-walled carbon nanotube bundles. Phys Rev Lett 2003;91(1):015504-1–4.
[30] LaBrosse MR, Shi W, Johnson JK. Adsorption of gases in carbon nanotubes: are defect interstitial sites important? Langmuir 2008;24(17):9430–9.
[31] Penza M, Tagliente MA, Aversa P, Cassano G. Organic-vapor detection using carbon-nanotubes nanocomposite microacoustic sensors. Chem Phys Lett 2005;409(4–6):349–54.
[32] Brukh R, Sae-Khow O, Mitra S. Stabilizing single-walled carbon nanotubes by removal of residual metal catalysts. Chem Phys Lett 2008;459(1–6):149–52.